Dihydrofolate reductase: Sequential resonance assignments using 2D and 3D NMR and secondary structure determination in solution

ARTICLE *in* BIOCHEMISTRY · JULY 1991

Impact Factor: 3.02 · DOI: 10.1021/bi00239a035 · Source: PubMed

9 AUTHORS, INCLUDING:

Jesús Jiménez-Barbero
Center for Cooperative Research in Biosciences
541 PUBLICATIONS **10,312** CITATIONS
SEE PROFILE

Vladimir Polshakov
Lomonosov Moscow State University
70 PUBLICATIONS **526** CITATIONS
SEE PROFILE

Gordon Roberts
University of Leicester
314 PUBLICATIONS **10,125** CITATIONS
SEE PROFILE

James Feeney
MRC National Institute for Medical Research
315 PUBLICATIONS **8,193** CITATIONS
SEE PROFILE

Dihydrofolate Reductase: Sequential Resonance Assignments Using 2D and 3D NMR and Secondary Structure Determination in Solution†

M. D. Carr,‡ B. Birdsall,‡ T. A. Frenkiel,§ C. J. Bauer,§ J. Jimenez-Barbero,‡ V. I. Polshakov,‡ J. E. McCormick,‡ G. C. K. Roberts,∥ and J. Feeney*,‡

Laboratory of Molecular Structure and Biomedical NMR Centre, National Institute for Medical Research, London NW7 1AA, U.K., and Department of Biochemistry University of Leicester, Leicester LE1 9HN, U.K.

Received November 7, 1990; Revised Manuscript Received February 8, 1991

ABSTRACT: Three-dimensional (3D) heteronuclear NMR techniques have been used to make sequential ^1H and ^{15}N resonance assignments for most of the residues of *Lactobacillus casei* dihydrofolate reductase (DHFR), a monomeric protein of molecular mass 18 300 Da. A uniformly ^{15}N-labeled sample of the protein was prepared and its complex with methotrexate (MTX) studied by 3D $^{15}N/^1H$ nuclear Overhauser-heteronuclear multiple quantum coherence (NOESY-HMQC), Hartmann-Hahn-heteronuclear multiple quantum coherence (HOHAHA-HMQC), and HMQC-NOESY-HMQC experiments. These experiments overcame most of the spectral overlap problems caused by chemical shift degeneracies in 2D spectra and allowed the ^1H-^1H through-space and through-bond connectivities to be identified unambiguously, leading to the resonance assignments. The novel HMQC-NOESY-HMQC experiment allows NOE cross peaks to be detected between NH protons even when their ^1H chemical shifts are degenerate as long as the amide ^{15}N chemical shifts are nondegenerate. The 3D experiments, in combination with conventional 2D NOESY, COSY, and HOHAHA experiments on unlabelled and selectively deuterated DHFR, provide backbone assignments for 146 of the 162 residues and side-chain assignments for 104 residues of the protein. Data from the NOE-based experiments and identification of the slowly exchanging amide protons provide detailed information about the secondary structure of the binary complex of the protein with methotrexate. Sequential NH_i-NH_{i+1} NOEs define four regions with helical structure. Two of these regions, residues 44-49 and 79-89, correspond to within one amino acid to helices C and E in the crystal structure of the DHFR·methotrexate·NADPH complex [Bolin et al. (1982) *J. Biol. Chem. 257*, 13650-13662], while the NMR-determined helix formed by residues 26-35 is about one turn shorter at the N-terminus than helix B in the crystal structure, which spans residues 23-34. Similarly, the NMR-determined helical region comprising residues 102-110 is somewhat offset from the crystal structure's helix F, which encompasses residues 97-107. Regions of β-sheet structure were characterized in the binary complex by strong αCH_i-NH_{i+1} NOEs and by slowly exchanging amide protons. In addition, several long-range NOEs were identified linking together these stretches to form a β-sheet. These elements align perfectly with corresponding elements in the crystal structure of the DHFR·methotrexate·NADPH complex, which contains an eight-stranded β-sheet, indicating that the main body of the β-sheet is preserved in the binary complex in solution.

Dihydrofolate reductase is a monomeric enzyme of molecular weight 18 300, which catalyzes the reduction of dihydrofolate to tetrahydrofolate using NADPH as coenzyme. The enzyme is of considerable pharmacological significance, since it is the target for "antifolate" drugs such as trimethoprim, methotrexate, and pyrimethamine. Over the last few years a substantial amount of structural information on various enzyme ligand complexes has been obtained, largely from X-ray crystallography and NMR studies [for reviews, see Blakley (1985), Freisheim and Matthews (1984), Feeney (1990), and Roberts (1990)]. This has led to the design of improved DHFR[1] inhibitors [see, for example, Kuyper et al. (1982) and Birdsall et al. (1984)].

NMR studies of DHFR·ligand complexes have proven particularly successful for obtaining detailed information about interactions, multiple conformations, and dynamic processes within the complexes (Birdsall et al., 1989a,b, 1990b). In order to extract such information, however, it is first necessary to assign resonances in the NMR spectra to specific nuclei in either the protein or the bound ligands. Much of our earlier work concentrated on studies of ligand resonances, since these could easily be assigned by selective isotopic labeling and magnetization transfer methods. Nuclei on the ligand are obviously good probes for monitoring dynamic processes and ionization states within the active site of the complex. However, in order to study protein-ligand interactions or conformational equilibria in detail, it is clearly necessary also to assign resonances from the protein. In previous studies (Hammond et al., 1986; Birdsall et al., 1990a), we have obtained side-chain resonance assignments for about 25% of the residues in *Lactobacillus casei* DHFR by correlating observed

† This work was supported by the Medical Research Council and the Wellcome Trust.

‡ Laboratory of Molecular Structure, National Institute for Medical Research.

§ Biomedical NMR Centre, National Institute for Medical Research.

∥ University of Leicester.

[1] Abbreviations: 2D, two dimensional; 3D, three dimensional; COSY, two-dimensional correlation spectroscopy; DHFR, dihydrofolate reductase; DQF-COSY, double-quantum-filtered correlation spectroscopy; enzymes, dihydrofolate reductase (EC 1.5.1.3); HMQC, heteronuclear multiple quantum coherence spectroscopy; HOHAHA, homonuclear Hartmann-Hahn spectroscopy; MTX, methotrexate; NOE, nuclear Overhauser effect; NOESY, two-dimensional nuclear Overhauser effect spectroscopy; TPPI, time-proportional phase incrementation.

0006-2960/91/0430-6330$02.50/0

NOEs with those predicted by the crystal structure of the DHFR·MTX·NADPH ternary complex (Bolin et al., 1982). This method relies on the assumption that the crystal and solution structures are similar. At that time, the sequential assignment method, which is based on correlating NOE data with sequence information (Wüthrich, 1986) could not easily be applied to proteins the size of DHFR (162 residues) due to severe ^1H chemical shift degeneracy.

The introduction of methods involving ^{15}N or ^{13}C isotope editing of ^1H spectra (McIntosh et al., 1987; Senn et al., 1987) has provided new possibilities for assigning ^1H spectra of larger proteins. Over the last few years several relayed 2D and 3D $^{15}N/^1H$ and $^{13}C/^1H$ NMR experiments have been developed and proved to be useful for assigning ^1H spectra of isotopically labeled proteins comparable in size to DHFR (Marion et al., 1989a; Zuiderweg & Fesik, 1989; Driscoll et al., 1990; Fesik & Zuiderweg, 1990). For example, Driscoll et al., (1990) have used 3D HOHAHA–HMQC and NOESY–HMQC experiments to make complete backbone assignments for interleukin 1β (152 residues) uniformly labeled with ^{15}N. Similarly, Torchia et al. (1989) have successfully extracted backbone assignments for 127 of the 149 residues of staphylococcal nuclease complexed with thymidine 3′,5′-diphosphate and Ca^{2+} by using extensive ^{15}N and ^{13}C labeling in conjunction with isotope-editing 2D experiments. Other workers have used the one-bond ^{13}C–^{15}N scalar coupling ($J_{^{13}CO-^{15}NH}$) between nuclei in adjacent amino acids to make direct sequential assignments independent of NOE data (Llinas et al., 1977; Westler et al., 1988; Stockman et al., 1989; Niemczura et al., 1989). This approach has been refined by Ikura et al. (1990), who have developed heteronuclear triple-resonance 3D pulse sequences to provide a general method of obtaining sequential assignments for proteins uniformly labeled with ^{15}N and ^{13}C, which they have applied to calmodulin. These triple-resonance methods all rely on multistep magnetization transfers via resolved one-bond J couplings and thus provide unambiguous sequential assignments for protein backbone resonances that are independent of backbone conformation. More recently, Kay et al. (1990) have introduced 4D heteronuclear triple-resonance experiments to assign fully the NOEs between NH and aliphatic protons in the spectrum of interleukin 1β.

In this present study we have applied 3D NOESY–HMQC and HOHAHA–HMQC experiments to uniformly ^{15}N-labeled dihydrofolate reductase (as its binary complex with methotrexate) in order to obtain sequential resonance assignments and to extract secondary structure information for the protein in solution. A novel HMQC–NOESY–HMQC experiment (Frenkiel et al., 1990) has also been used to overcome problems arising from NH chemical shift degeneracy, which would otherwise have prevented us from fully defining the secondary structural elements.

Materials and Methods

Unlabeled *L. casei* DHFR was prepared as described previously from an *Escherichia coli* strain into which the structural gene for the *L. casei* enzyme had been cloned (Dann et al., 1976; Andrews et al., 1985). In the case of the ^{15}N-labeled protein, however, the *E. coli* cells were grown up on a minimal medium containing 10 g/L glucose, 1 g/L sodium citrate, 20 g/L potassium phosphate, 0.2 g/L magnesium sulfate, 40 mg/L L-tryptophan, 50 mg/L ampicillin, and 1 g/L 99% ^{15}N-enriched ammonium sulfate. (L-Tryptophan was included in the growth medium since the *E. coli* strain used is auxotrophic for tryptophan; however, complete ^{15}N labeling of the tryptophan amide nitrogen occurred as a result of transaminase activity.)

The 99% ^{15}N-enriched ammonium sulfate was obtained from Cambridge Isotope Laboratories, while 100 atom % D_2O and methotrexate were purchased from Sigma. All other reagents used were of analytical reagent quality.

The NMR experiments were carried out on 0.5-mL samples of 3–5 mM DHFR·MTX in 500 mM potassium chloride and 50 mM potassium phosphate buffer, pH* 6.5 or 4.1 made up with either D_2O, or 90% H_2O/10% D_2O, as appropriate (pH* values are pH meter readings uncorrected for deuterium isotope effects). In order to detect signals from the slowly exchanging amide protons, samples of DHFR·MTX were lyophilized from H_2O and then taken up in D_2O just prior to carrying out the 2D NMR measurements.

The majority of the ^1H and all $^{15}N/^1H$ NMR experiments were performed on a Bruker AM500 spectrometer, but a few ^1H measurements were also made on an AM400. The 2D and 3D spectra were all acquired in the phase-sensitive mode, with the TPPI method being used to achieve quadrature detection in the indirectly detected frequency dimensions (Marion & Wüthrich, 1983). Good spectral baselines needing no additional software-based corrections were obtained by using the procedure described previously (Frenkiel et al., 1990). NMR experiments were performed at either 30 or 35 °C. DQF-COSY spectra (Rance et al., 1983), HOHAHA (Davis & Bax, 1985; Braunschweiler & Ernst, 1983) with spin-lock times of 40–90 ms, and NOESY (Jeener et al., 1979; Macura et al., 1981) with mixing times from 15 to 200 ms were recorded from both D_2O and H_2O samples of DHFR·MTX. The $^{15}N/^1H$ experiments carried out were HMQC (Mueller, 1979; Bax et al., 1983), 3D HOHAHA–HMQC (Marion et al., 1989a) with a spin-lock time of 50 ms, 3D NOESY–HMQC (Marion et al., 1989b), and 3D HMQC–NOESY–HMQC (Frenkiel et al., 1990). The 3D NOESY–HMQC and HMQC–NOESY–HMQC spectra were both acquired by using a 100-ms NOE buildup period. In the HMQC sections of the 2D and 3D $^{15}N/^1H$ experiments, the delays needed to allow evolution of the single-bond ^{15}N–^1H coupling were set to 5 ms. The spin-lock field in the HOHAHA and 3D HOHAHA–HMQC experiments was produced by using an MLEV17 sequence (Bax & Davis, 1985) with a spin-lock field of approximately 7.5 kHz.

Water suppression in both 2D and 3D experiments was achieved by the use of selective presaturation, with either continuous wave irradiation or a DANTE sequence (Morris & Freeman, 1978). To prevent the recovery of solvent signal during the mixing time of NOESY-based experiments, a 180° proton pulse was applied at the center of this period. In order to observe signals involving αCH protons resonating at or very close to the chemical shift of the water, many of the 2D and 3D experiments employed a 60-ms SCUBA sequence immediately after the presaturation period to allow the restoration of magnetization to the bleached αCH protons by cross relaxation from neighboring protons (Brown et al., (1988)).

The spectra from 2D NMR experiments were typically acquired over 1–3 days, collecting 512 t_1 increments, 64–192 scans per increment, and 4096 points per scan. For spectra recorded from D_2O samples of DHFR·MTX the spectral width was set to 12.8 ppm in both dimensions, while for H_2O samples a value of 14.0 ppm was used. The 3D $^{15}N/^1H$ spectra were recorded over 3.5–4 days, acquiring 126 × 64 increments for the NOESY–HMQC, 114 × 64 increments for the HOHAHA–HMQC, and 84 × 84 increments for the HMQC–NOESY–HMQC, 16–32 transients per increment, and 512 points per transient. In the NOESY–HMQC and HOH-

AHA–HMQC experiments the spectral widths in F_1, F_2, and F_3 were 13.9, 35.3, and 7.1 ppm, respectively. The spectral widths used for the HMQC–NOESY–HMQC experiment were 35.3 ppm in F_1 and F_2 and 7.1 ppm in F_3.

Processing of 2D data was carried out by using standard Bruker NMR software. The original data were usually zero-filled once in F_2 and twice in F_1, while mild resolution enhancement was achieved by applying shifted sine or sine-squared apodization functions in both dimensions.

The 3D data were transformed, displayed, and plotted by using software written in-house. In the NOESY–HMQC and HOHAHA–HMQC experiments, the data were zero-filled once in all dimensions and a sine-squared window function shifted by $\pi/2$, $\pi/4$, and $\pi/2$ was applied in F_1, F_2, and F_3 respectively. The HMQC–NOESY–HMQC data were treated similarly, except that the sine-squared function used was shifted by $\pi/3$ in F_1, $\pi/3$ in F_2, and $\pi/2$ in F_3.

Results and Discussion

(*i*) *Spin-System Assignments.* The first stage in the assignment of protein ^{1}H NMR spectra is the identification of groups of resonances that form single amino acid spin systems and assignment of these to particular types, or classes, of amino acid residues. For small proteins this has been achieved by observing the scalar through-bond connectivities detected in experiments such as 2D COSY and HOHAHA, since specific types or classes of amino acids give rise to characteristic connectivity patterns (Wüthrich, 1986). However, these procedures are more difficult to apply to larger proteins because of the severe overlap of cross peaks in some regions of the 2D spectra and also because many of the expected cross peaks are unobservable if the signal line widths are larger than the scalar coupling constants active in coherent magnetisation transfer. Such problems are encountered when proteins the size of *L. casei* DHFR (M_r = 18 300) are examined. For example, in spectra of the DHFR·MTX complex, COSY-type cross peaks could only be observed from 147 of the 154 backbone and eight arginine side-chain NH protons. In addition, there is severe overlap of cross peaks in 2D DQF-COSY and HOHAHA spectra, particularly in the aliphatic–aliphatic region. These problems severely limit the identification of complete connectivity patterns in spectra, particularly for long-chain amino acids: thus, for the DHFR·MTX complex it proved possible to obtain complete spin-system assignments for only 59 residues and partial assignments for another 15, as described below.

Despite the problems outlined above, the spin systems for some types of residues, in particular alanine and threonine, could be assigned with relative ease. On the basis of the connectivities and cross-peak structures observed in 2D DQF-COSY, HOHAHA, and 3D ^{15}N/^{1}H HOHAHA–HMQC, it was possible to make complete spin-system assignments for 13 of the 15 alanines and for 12 out of 14 threonines. The nonexchangeable protons of one additional alanine and the two remaining threonines were also identified.

The spin systems of valine residues in the DHFR·MTX complex proved to be more difficult to identify by this approach, and it was possible to identify only 11 complete valine spin systems and partially assign one other from the 2D and 3D spectra. However, after analysis of DQF-COSY and HOHAHA spectra recorded from specifically labeled DHFR samples, where either the methyl or the α protons of valine residues are deuterated, 15 of the 16 valine spin systems could be fully characterized (Feeney et al., 1990). In two cases there were no detectable αCH–βCH COSY cross peaks, or relay

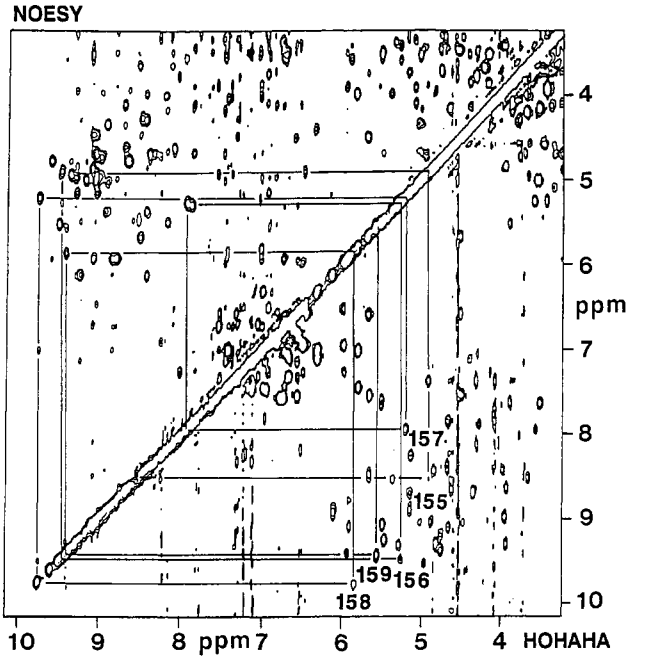

FIGURE 1: Parts of the 2D NOESY and HOHAHA spectra of DHFR·MTX obtained from a sample freshly dissolved in ^2H_2O so that NH resonances are observed only for slowly exchanging NHs. The sequential αN NOEs for residues 155–159 in the NOESY spectrum (above the diagonal) are shown connected to the appropriate NH–αCH cross peaks in the HOHAHA spectrum (below the diagonal).

peaks involving the NH resonances and the backbone and side-chain protons could only be associated with each other by using NOEs from the NH protons to the β, γ, and γ' protons. Only 15 of the 16 valine residues in the DHFR·MTX complex produced detectable through-bond NH–αCH cross peaks; hence, assignments for the remaining valine were limited to the nonexchangeable protons.

Glycine residues also form unique spin systems that should be readily detectable from 2D and 3D spectral connectivities. Where the signals arising from their two α protons are well separated, they can be easily identified from the intense antiphase square array of α–α' cross peaks with large J splittings observed in DQF-COSY spectra of samples dissolved in D_2O. In the case of the DHFR·MTX complex, 7 of the 10 glycine spin systems could be recognized in this way, but only four of these could be traced back to the NH signal.

In addition to the spin-system assignments described so far it was possible by using the same methodology to identify 15 of the 46 AMX systems, one isoleucine spin system from the NH to γ methyl group, and six spin systems from residues having side-chain connectivities extending from the NH to at least the γ position. Thus, a total of 66 through-bond NH–αCH cross peaks were assigned to specific types or classes of amino acid residues and could therefore be used as anchor points in the sequential assignment of the DHFR·MTX spectrum. These are in addition to the side-chain proton assignments made previously for the 25 aromatic amino acid residues by using a combination of selective deuteration and 2D NMR (Hammond et al., 1986; Birdsall et al., 1990a). The assigned aromatic side-chain signals (Birdsall et al., 1990a) were used to confirm sequential assignments for the backbone resonances by identifying NOEs from NH, αCH, and βCH resonances to the aromatic ring protons.

(*ii*) *Sequence-Specific Assignments.* The sequential assignment procedure developed by Wüthrich and co-workers provides a general method of obtaining essentially complete

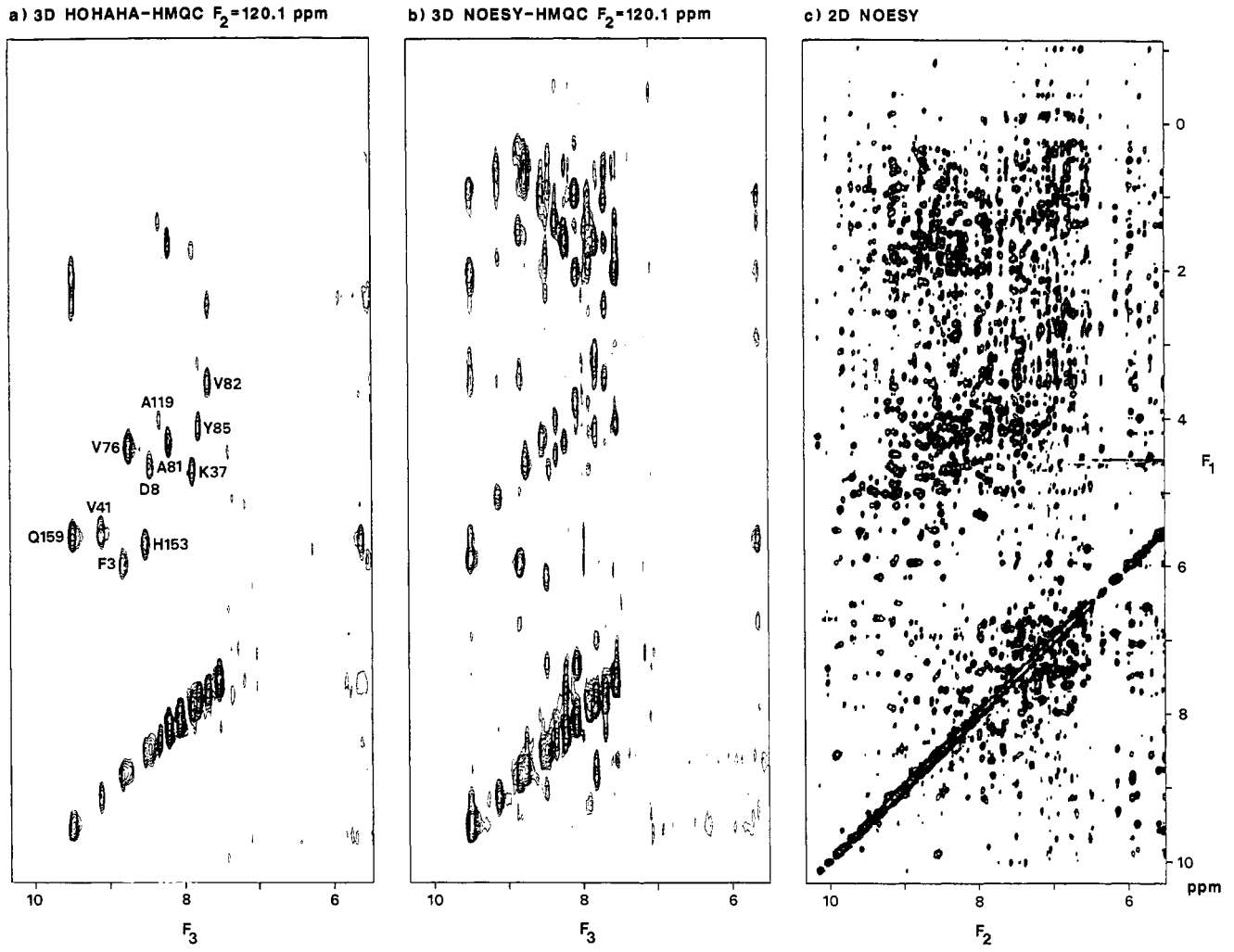

FIGURE 2: Comparison between a 2D NOESY spectrum and identical regions from F_1–F_3 cross sections of 3D $^{15}N/^1H$ NOESY–HMQC and HOHAHA–HMQC experiments for the uniformly ^{15}N-labeled DHFR·MTX complex. In the F_2 (^{15}N) slice from the HOHAHA–HMQC spectrum the assignments are given for the NH–αCH cross peaks. The F_1–F_3 cross sections shown are among the most complicated but still contain cross peaks from only 11 backbone amide protons, with no NH shift degeneracy. The 3D NOESY–HMQC slice is clearly much simpler and more amenable to analysis than the corresponding region from the 2D NOESY spectrum.

sequence-specific assignments for complex protein ^1H NMR spectra based purely on correlating amino acid sequence and NMR data (Wagner & Wüthrich, 1982; Wüthrich, 1986). The heart of the procedure is the concept of identifying spin systems that follow one another in the sequence, thereby building up a number of continuous stretches of adjacent spin systems, which can be matched to segments of the known protein sequence in order to obtain the sequence-specific resonance assignments. The amino acid spin systems can be identified as originating from neighboring residues by observation of NOEs between protons in residues i and $i + 1$ in 2D NOESY or ROESY spectra. Particularly important in this respect are NOEs involving the exchangeable NH protons, specifically NH–NH (NN), αCH–NH (αN), and βCH–NH (βN) NOEs. This approach works extremely well and has resulted in the near complete assignment of the ^1H NMR spectra of many proteins with molecular weights below 15 000 (Strop et al., 1983; Carver et al., 1986; Widmer et al., 1988; Redfield & Dobson, 1988; Clore et al., 1989; Breg et al., 1989). However, for somewhat larger proteins, such as DHFR, problems arise as a direct consequence of the increased number of resonances present in the ^1H spectra. This results in severe cross-peak overlap in key areas of 2D NOESY spectra, such as in the NH–αCH and NH–βCH regions of the DHFR·MTX spectrum, and means that there are many completely, or nearly degenerate, NH, αCH, and βCH signals. These problems preclude the identification of many sequential NOEs in 2D NOESY spectra of the DHFR·MTX complex.

Problems of cross-peak overlap do occur in spectra of many small proteins, but generally these are less severe and can be overcome by recording several complete sets of 2D data, either at different temperatures or from samples adjusted to various pH values, in order to take advantage of the differential sensitivity of signals to changes in pH or temperature. Alternatively, simpler 2D spectra can be obtained from protein samples that have been freshly dissolved in D_2O, where only slowly exchanging NHs will produce cross peaks. Both of these strategies were actively pursued in initial attempts to obtain sequential assignments for DHFR·MTX, but although reasonably successful they only provided a partial solution to the problems of cross-peak overlap and signal degeneracy. There is only limited scope for varying the sample conditions since the concentration of DHFR·MTX required for many of the ^1H NMR studies is around 5 mM, at which the enzyme is stable up to about 35 °C and over a pH range from 4 to 8. The quality of the 2D spectra obtained from DHFR·MTX samples deteriorates markedly when the experiments are carried out much below 35 °C, primarily due to increased signal line widths; thus, varying the sample temperature was of little help in making assignments. However, DQF-COSY

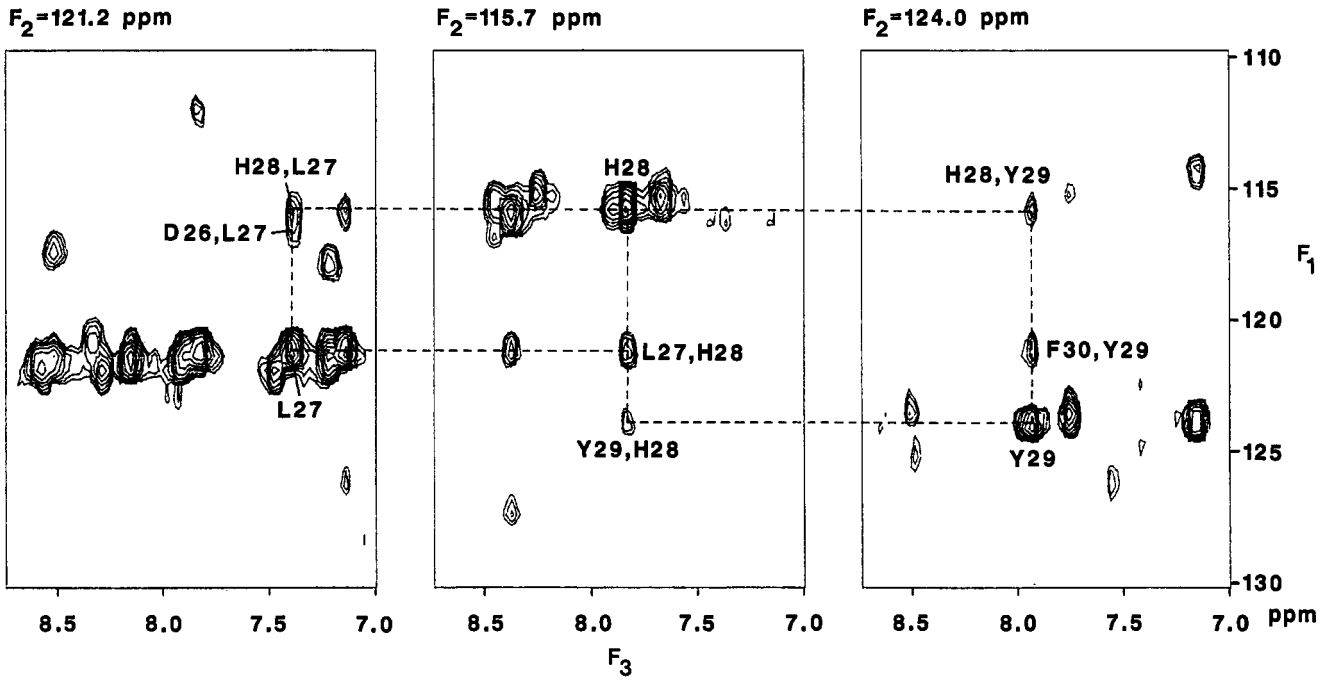

FIGURE 3: Representative F_2 (^{15}N) slices from a $^{15}N/^1H$ HMQC-NOESY-HMQC spectrum of DHFR·MTX taken at the amide ^{15}N shifts of Leu 27, His 28, and Tyr 29. The labeled cross peaks arise from the sequential NH-NH NOEs linking neighboring residues in the sequence. In the HMQC-NOESY-HMQC experiment, cross peaks arising from NH-NH NOEs are characterized by the ^{15}N shifts of both amide nitrogens and the ^1H shift of the amide proton to which NOE transfer has occurred. Hence, the experiment can detect NOEs between NHs with identical or quite similar ^1H shifts (see text); these NOEs cannot be detected in 2D NOESY or 3D NOESY-HMQC spectra. This situation occurs for the NH-NH NOE between His 28 and Tyr 29, where the shift difference between the two amide protons is only 0.1 ppm.

and NOESY spectra recorded from a sample adjusted to pH 4.1 were very useful in resolving some of the ambiguities caused by αCH degeneracy in 2D and 3D spectra acquired from samples at the standard pH of 6.5. The HOHAHA and NOESY spectra obtained from DHFR·MTX freshly dissolved in D_2O also proved surprisingly useful since the cross-peak overlap in regions involving NH resonances was much reduced, as a consequence of just 47 of the 162 amide protons persisting for over 24 h. Moreover, it was also possible to identify several stretches of residues linked by continuous αN sequential NOEs, as illustrated in Figure 1, which could be extended further by comparison with NOESY spectra obtained in H_2O.

Detailed analysis of all the 2D data enabled us to obtain firm sequence-specific assignments for about 40% of the protein residues. Hence, the majority of the assignments reported here have relied upon the preparation of ^{15}N-labeled DHFR and the use of 3D heteronuclear NMR to overcome the overlap and signal degeneracy present in 2D spectra. Two 3D $^{15}N/^1H$ experiments used in the assignment of DHFR·MTX were HOHAHA-HMQC (Marion et al., 1989a) and NOESY-HMQC (Marion et al., 1989b). These experiments can be thought of as generating ^{15}N-edited HOHAHA or NOESY spectra, with signals spread out in a third dimension according to the ^{15}N shift of the amide nitrogens. Thus, since 3D $^{15}N/^1H$ HOHAHA-HMQC and NOESY-HMQC spectra contain the same number of peaks as 2D ^{15}N-edited HOHAHA and NOESY experiments, slices of the 3D spectra taken at particular ^{15}N frequencies correspond to subsets of the 2D data set. Consequently there is much less overlap of cross peaks in the 3D slices, as illustrated in Figure 2. There is only a single example in DHFR·MTX of two NH signals that are still degenerate in the 3D spectra. However, all the ambiguities caused by αCH and βCH chemical shift degeneracy remain in the 3D spectra.

A novel 3D $^{15}N/^1H$ experiment termed HMQC-NOESY-HMQC was also carried out on the ^{15}N-labeled DHFR·MTX complex in order to detect NOEs between NH protons (Frenkiel et al., 1990). In these spectra the NOE connections between amide protons directly bonded to ^{15}N nuclei give rise to cross peaks that are characterized by the ^{15}N shifts of both amide nitrogens involved and by the ^1H shift of the proton to which NOE transfer has occurred. Thus, the HMQC-NOESY-HMQC experiment was particularly valuable because it enabled us to identify sequential NH-NH NOEs between amide protons with identical or closely similar ^1H shifts as long as the amide ^{15}N shifts are distinct. It should be noted that in the 2D NOESY and 3D NOESY-HMQC spectra of DHFR·MTX it was impossible to identify NOE cross peaks between NH proton signals that were separated by less than about 0.1 ppm, since they simply merged with the diagonal peaks. This situation occurs for the NH-NH NOEs connecting valine 79 to alanine 80, tyrosine 46 to glutamate 47, histidine 28 to tyrosine 29, and alanine 32 to glutamine 33. The sequential assignments of residues 26–37 rely upon the NH-NH NOEs from histidine 28 to tyrosine 29 and from alanine 32 to glutamine 33, and therefore the resonances from this part of the protein could not have been assigned without the 3D HMQC-NOESY-HMQC spectra. Figure 3 shows three F_2 (^{15}N) slices from an HMQC-NOESY-HMQC experiment at the ^{15}N shifts of the leucine 27, histidine 28, and tyrosine 29 amide nitrogens: the NOE cross peaks between the amide protons of residues 28 and 29 are clearly seen in the spectra.

The procedure for making sequential assignments of proteins by using 3D NOESY-HMQC, HMQC-NOESY-HMQC, and HOHAHA-HMQC spectra is basically the same as with 2D NOESY and HOHAHA data. Thus, it is simply a matter of trying to identify αN, NN, and βN NOEs in the NOESY-HMQC and HMQC-NOESY-HMQC spectra, while using the 3D HOHAHA-HMQC spectrum to obtain the amide nitrogen ^{15}N shifts and to confirm the NH, αCH, and βCH ^1H shifts of the amino acid spin systems identified

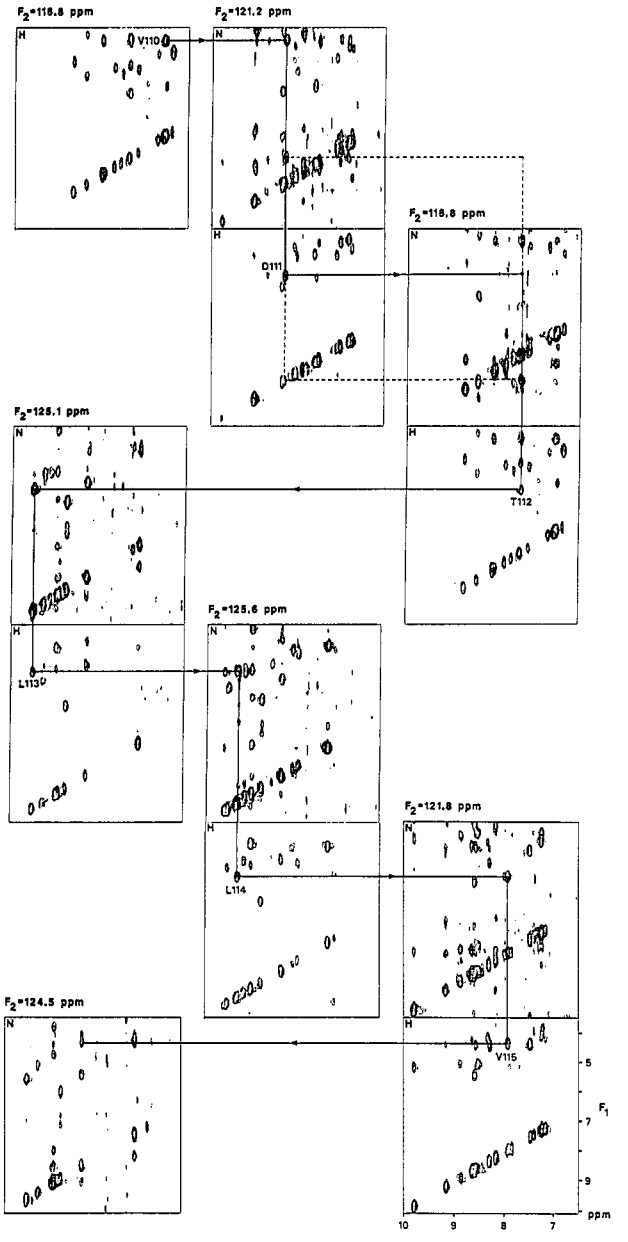

FIGURE 4: Series of F_1–F_3 cross sections from $^{15}N/^1H$ HOHAHA–HMQC spectra (labeled H) and NOESY–HMQC spectra (labeled N) of DHFR·MTX illustrating the sequential assignment of Val 110–Thr 116 via sequential αCH–NH (solid lines) and NH–NH (dashed lines) NOEs. The assignments of the NH–αCH scalar cross peaks for Val 110–Val 115 are given in the appropriate HOHAHA–HMQC F_2 slices. The procedure for making sequential assignments of proteins by using 3D NOESY–HMQC and HOHAHA–HMQC spectra is basically the same as with 2D data. Thus, NH–NH, αCH–NH, and βCH–NH NOEs are identified in the NOESY–HMQC spectrum, while the HOHAHA–HMQC spectrum is used as a guide to the amide nitrogen ^{15}N shifts and NH, αCH, and βCH ^1H shifts of the amino acid spin systems identified previously.

previously. To illustrate the process, the steps leading to the assignment of the resonances of residues 110–116 are shown in Figure 4.

The αN connectivities for DHFR·MTX were identified by searching through the 64 ^{15}N (F_2) slices of the NOESY–HMQC spectrum in order to find all the possible αCH–NH NOEs at the shift of the αCH of interest. In cases where the αCH proton being considered has a shift similar to several other αCHs, it was advantageous to pick out the corresponding NOEs in the 2D NOESY spectrum, if possible, since the better resolution in the F_1 dimension often allowed one to decide whether the observed NOEs were from the αCH of interest. Also, by adopting this strategy it was possible to make use of the 2D spectra acquired from a sample adjusted to pH 4.1 to resolve some of the ambiguities in the 3D NOESY–HMQC spectrum caused by αCH shift degeneracy at pH 6.5. An alternative way of solving the αCH degeneracy problem was to identify additional sequential NOEs for the same assignment step, which support only one of the αN possibilities.

The tracing of NH–NH NOEs in the 3D spectra of the DHFR·MTX complex was relatively straightforward. To determine whether a particular NH resonance showed NOEs to other amide protons, it was simply a matter of examining the appropriate ^{15}N (F_2) slices from the NOESY–HMQC and HMQC–NOESY–HMQC spectra to see if any cross peaks appeared at the correct NH ^1H shift. If one or more NH–NH NOEs were identified, then the ^{15}N and ^1H shifts of the NHs from which NOE transfer had occurred could be obtained directly from the HMQC–NOESY–HMQC and NOESY–HMQC slices, respectively. Due to the reciprocal nature of the cross-relaxation processes, the existence of the NOEs could be confirmed by picking out the corresponding cross peaks in ^{15}N slices taken at these amide nitrogen ^{15}N shifts.

The βN NOEs observed for DHFR·MTX were picked out after the identification of either αN or NN connections between resonances in adjacent amino acid residues and so were used to provide supporting evidence for sequential assignment pathways rather than to make initial pairings of possible neighboring spin systems. Consequently no exhaustive search was made through the entire 3D NOESY–HMQC spectrum in order to identify all possible βCH–NH NOEs at specific βCH frequencies. This strategy was adopted because of the significant cross-peak overlap and degeneracy of side-chain signals in the region of the NOESY–HMQC spectrum that contains the βN NOEs, which meant that in many cases it was impossible to identify βN NOEs unequivocally.

Despite some remaining ambiguities in the 3D NOESY–HMQC spectrum, caused mainly by the overlap of signals from nonexchangeable protons, a detailed analysis of the 3D data allowed us to identify a substantial number of sequential NOEs, which are summarized in Figure 5. Hence, it was possible to obtain sequential resonance assignments for 147 of DHFR's 162 residues, details of which are given in Table I.

It is important to consider why assignments were not obtained for the remaining 15 amino acids. Five of these are proline residues, which are notoriously difficult to assign, the main problem being the severe cross-peak overlap in the aliphatic region of DQF-COSY or HOHAHA spectra, which prevents identification of the proline spin systems. Thus, sequence-specific assignments for proline residues depend upon the identification of sequential αN, αδ, or δN NOEs. However, cross-peak overlap in the aliphatic region of NOESY spectra precluded the identification of αδ connections, and possible αN or δN NOEs could only be attributed to proline residues when the αCH or δCH resonances were nondegenerate with other proton signals. The specific problems associated with making proline assignments could almost certainly be overcome by preparing completely ^{13}C-labeled DHFR and by using the recently developed 3D $^{13}C/^1H$ HCCH-COSY (Bax et al., 1990a) and HCCH-TOCSY (Bax et al., 1990b) experiments to fully characterize the spin systems from "long-chain" amino acid residues, such as proline. Torchia et al. (1989) have already made assignments for prolines in staphylococcal nuclease after incorporating [2-^{13}C]proline.

Examination of the crystal structure of the DHFR·MTX·NADPH complex revealed that all the residues other

Table I: ^{1}H and ^{15}N Resonance Assignments for the *L. casei* DHFR·MTX Complex[a]

		^{15}N	NH	α	α′	β	β′	γ	γ′	δ	δ′	other
1	Thr			3.77		3.68		0.23				
2	Ala	131.80	8.77	5.95		1.51						
3	Phe	120.30	8.82	5.95		3.49	3.24					6.77 (2,6), 7.02 (3,5), 7.44 (4)
4	Leu	125.25	8.89	6.15		2.01		2.32		1.14	0.49	
5	Trp	128.05	9.29	5.51								11.07 (H1), 6.29 (H2), 7.16 (H4), 6.70 (H5), 6.60 (H6), 7.36 (H7)
6	Ala	121.70	8.57	5.40		2.37						
7	Gln	114.75	8.97	6.15								
8	Asp	120.20	8.46	4.64								
9	Arg	115.35	7.66									
10	Asp	118.75	8.42	4.99		2.92	2.63					
11	Gly	107.20	7.94	4.55	3.46							
12	Leu	124.55	9.03	4.34				1.67		0.90	0.77	
13	Ile	112.10	8.94	5.18		2.34						1.31 (γ-Me)
14	Gly	106.50	7.49	4.32	3.77							
15	Lys	122.10	8.54	4.35		1.41						
16	Asp	129.35	10.12	4.23		2.88	2.38					
17	Gly	104.50	8.98	3.94	3.45							
18	His	117.65	7.81	4.93		3.67						8.39 (H2), 7.19 (H4)
19	Leu							1.38		0.63	0.43	
20	Pro											
21	Trp											9.67 (H1), 6.49 (H2), 6.00 (H4), 6.53 (H5), 7.30 (H6), 6.97 (H7)
22	His											7.88 (H2), 7.21 (H4)
23	Leu							1.02		0.62	0.04	
24	Pro											
25	Asp											
26	Asp	116.45	6.93	5.33								
27	Leu	121.15	7.37	3.86				1.44		0.61	-0.02	
28	His	115.70	7.82									8.39 (H2), 7.38 (H4)
29	Tyr	123.85	7.91	4.14		3.04						6.75 (2,6), 6.64 (3,5)
30	Phe	121.05	9.12									6.72 (2,6), 7.10 (3,5), 7.35 (4)
31	Arg	121.55	8.14	3.66								
32	Ala	121.10	7.81	3.91		1.34						
33	Gln	111.95	7.89	4.08								
34	Thr	105.80	7.31	4.16		4.41		1.19				
35	Val	120.45	8.06	3.76		2.02		0.96	0.96			
36	Gly	111.35	9.19	4.17	3.86							
37	Lys	120.25	7.88	4.70		1.73						
38	Ile			4.11								1.70 (γ-Me)
39	Met	129.30	8.73	5.18								2.14 (ε-Me)
40	Val	128.60	9.08	5.05		1.80		0.67	0.58			
41	Val	119.70	9.11	5.52		2.31		1.21	0.92			
42	Gly	105.85	8.19									
43	Arg											
44	Arg	116.90	8.23	3.84								
45	Thr	118.70	7.80	3.70		4.00		1.08				
46	Tyr	123.20	8.23	2.83		2.77						6.92 (2,6)
47	Glu	112.15	7.99	3.56		1.82						
48	Ser	114.35	7.41	4.34								
49	Phe	123.80	7.14	4.40								6.35 (2,6), 7.03 (3,5), 7.14 (4)
50	Pro											
51	Lys	116.35	6.80	4.25								
52	Arg	118.80	7.99	4.35		1.28						
53	Pro											
54	Leu							1.11		0.33	-0.10	
55	Pro			4.48								
56	Glu	112.70	9.05	3.87								
57	Arg	112.45	7.71	4.63								
58	Thr	118.90	8.37	4.36		4.10		1.09				
59	Asn	126.95	9.64	5.01		3.09						
60	Val	125.90	9.22	4.79		1.82		0.57	0.34			
61	Val	126.50	8.68	4.63		1.52		0.34	-0.16			
62	Leu	128.45	8.14	4.72				1.15		0.63	0.40	
63	Thr	119.60	8.43	4.70		3.70		0.89				
64	His					3.35	3.24					8.31 (H2), 7.26 (H4)
65	Gln	121.95	8.30	4.10								
66	Glu	127.20	8.68	3.27								
67	Asp	115.90	8.37	4.64		2.70						
68	Tyr	121.10	7.14	4.12		2.88	2.57					6.85 (2,6), 6.59 (3,5)
69	Gln	126.00	7.54	4.27		1.68						
70	Ala	126.35	7.26	4.31		0.99						
71	Gln	123.50	8.49	4.03								
72	Gly	107.75	8.13	4.07								
73	Ala	122.90	7.91	4.79		1.10						
74	Val	122.95	8.68	3.94		1.67		0.59	0.42			

Table I (Continued)

		^{15}N	NH	α	α′	β	β′	γ	γ′	δ	δ′	other
75	Val	127.50	8.36	4.60		1.93		0.81	0.76			
76	Val	120.00	8.74	4.39		2.15		0.64	0.51			
77	His	113.70	8.73	5.45		3.49	3.01					8.30 (H2), 7.29 (H4)
78	Asp	114.65	7.30	4.62								
79	Val	119.15	8.28	3.39		1.79		0.57	0.57			
80	Ala	123.05	8.34	4.30		1.50						
81	Ala	120.20	8.20	4.31		1.63						
82	Val	119.70	7.66	3.50		2.46		1.07	0.76			
83	Phe	117.65	7.85	4.50								7.36 (2,6), 7.36 (3,5)
84	Ala	122.40	8.63	4.22		1.56						
85	Tyr	120.00	7.80	4.10		3.22						6.97 (2,6), 6.53 (3,5)
86	Ala	122.60	8.84	3.95		1.72						
87	Lys	117.80	8.17	4.05		1.97						
88	Gln	114.40	7.22	3.11		1.43						
89	His	117.45	7.50	4.78		3.43	2.68					8.24 (H2), 6.57 (H4)
90	Pro			3.42								
91	Asp	116.60	8.82	4.52		2.70						
92	Gln	119.00	7.81	4.83		2.22						
93	Glu	121.90	7.27	4.37		1.78		2.35				
94	Leu	122.70	8.46	4.95		1.60		1.45		0.75	0.75	
95	Val	126.50	9.42	4.79		1.85		0.90	0.83			
96	Ile	127.85	9.67	4.47		2.56		0.88	1.43	-0.12		0.51 (γ-Me)
97	Ala	128.40	9.13	5.95		1.68						
98	Gly	102.45	5.95	4.18								
99	Gly	107.90	7.79	4.02	3.72							
100	Ala	123.95	8.99	3.95		1.46						
101	Gln											
102	Ile	121.40	7.21	3.79		1.80						0.66 (γ-Me)
103	Phe	117.80	7.68	4.00		2.70	2.50					5.83 (2,6), 7.04 (3,5), 7.49 (4)
104	Thr	114.10	8.27	3.70		4.19		1.22				
105	Ala	122.20	7.22	4.07		1.28						
106	Phe	112.30	7.41	4.95		3.82	2.93					7.60 (2,6), 6.78 (3,5), 6.82 (4)
107	Lys	120.35	7.51	4.04								
108	Asp	117.95	8.59	4.77		2.78	2.51					
109	Asp	118.00	7.95	4.90		3.07	2.64					
110	Val	117.15	6.97	3.84		1.23		0.35	0.35			
111	Asp	121.45	8.50	4.98		2.97	2.70					
112	Thr	117.30	7.66	5.54		3.90		1.38				
113	Leu	125.15	9.57	4.99				0.88		0.27	-0.99	
114	Leu	125.75	9.36	5.32		2.56		1.75		1.04	0.95	
115	Val	121.60	7.90	4.29		0.59		0.59	-0.05			
116	Thr	124.85	8.46	4.87		3.99		0.51				4.94 (OH)
117	Arg	127.00	9.14	4.69		1.26						
118	Leu	129.60	9.10	4.48				0.87		-0.36	-0.55	
119	Ala	120.60	8.33	4.01		1.33						
120	Gly	103.25	8.09	4.17	3.50							
121	Ser	111.70	7.61	5.02		3.54						
122	Phe	126.25	9.64	4.72		3.32	2.84					7.50 (2,6), 7.17 (3,5), 6.98 (4)
123	Glu											
124	Gly											
125	Asp	115.50	8.43	4.93								
126	Thr	116.75	7.68	4.63		3.73		1.20				
127	Lys	128.00	8.75	5.05		1.68						
128	Met	119.20	8.75	4.07								-0.37 (ε-Me)
129	Ile	117.35	7.10	4.30		1.93		1.28	0.59	0.76		1.09 (γ-Me)
130	Pro			4.43								
131	Leu	121.95	7.46	4.32		0.47	0.20	1.23		0.41	-0.05	
132	Asn	118.90	8.80	4.97		3.01	2.68					
133	Trp	123.60	7.74	3.75		3.17	2.67					10.00 (N1), 7.37 (H2), 5.70 (H4), 4.53 (H5), 6.60 (H6), 7.61 (H7)
134	Asp	115.15	8.24	4.75		2.82	2.71					
135	Asp	117.45	7.98	4.74		2.71	2.49					
136	Phe	118.40	8.30	5.17								6.95 (2,6), 6.85 (3,5)
137	Thr	114.95	9.35	4.85		3.94		1.16				
138	Lys	131.10	8.53	3.57								
139	Val	125.60	9.09	4.20		2.11		0.92	0.88			
140	Ser	112.55	7.44	4.58								
141	Ser	114.85	8.03	5.27		3.59	3.43					
142	Arg	125.45	8.48	4.72		1.86						
143	Thr	124.10	9.02	4.75		3.76		0.85				
144	Val	129.95	9.02	3.96		0.63		0.90	0.81			
145	Glu	126.55	8.48	4.44		1.80		2.11				
146	Asp	126.15	8.15	4.84		3.07						
147	Thr	117.75	7.87	3.87		4.09		1.25				
148	Asn	122.10	9.79	5.10		3.31	2.81					

Table I (Continued)

		^{15}N	NH	α	α'	β	β'	γ	γ'	δ	δ'	other
149	Pro											
150	Ala	118.95	7.66	3.92		1.34						
151	Leu	112.05	8.12	4.32		1.96		1.58		1.12	0.82	
152	Thr	124.90	7.40	4.25		4.16		1.09				
153	His	119.95	8.51	5.70		2.65	2.08					9.48 (H2), 5.98 (H4)
154	Thr	116.80	8.55	4.96		3.66		1.01				
155	Tyr	125.60	9.09	4.92		2.63						6.49 (2,6), 6.59 (3,5)
156	Glu	123.45	9.53	5.30		2.35						
157	Val	122.80	7.97	5.23		1.98		0.91	0.91			
158	Trp	127.30	9.82	5.89		3.10						11.12 (N1), 7.03 (H2), 7.46 (H4), 7.42 (H5), 7.15 (H6), 7.23 (H7)
159	Gln	120.25	9.48	5.60		2.18	1.99	2.53	2.43			
160	Lys	126.90	8.75	3.75								
161	Lys	126.60	8.50	4.11		1.57						
162	Ala	130.70	7.86	4.10		1.28						

[a] The ^{1}H chemical shifts (ppm) are referenced to DSS (sodium 4,4-dimethyl-4-silapentane-1-sulfonate). The ^{15}N chemical shifts (ppm) are on an arbitrary scale with the highest field NH_2 ^{15}N resonance assigned a shift of 108.00 ppm. Chemical shift values that are underlined are for resonances that were assigned only on the basis of correlations of NOE and X-ray structural data.

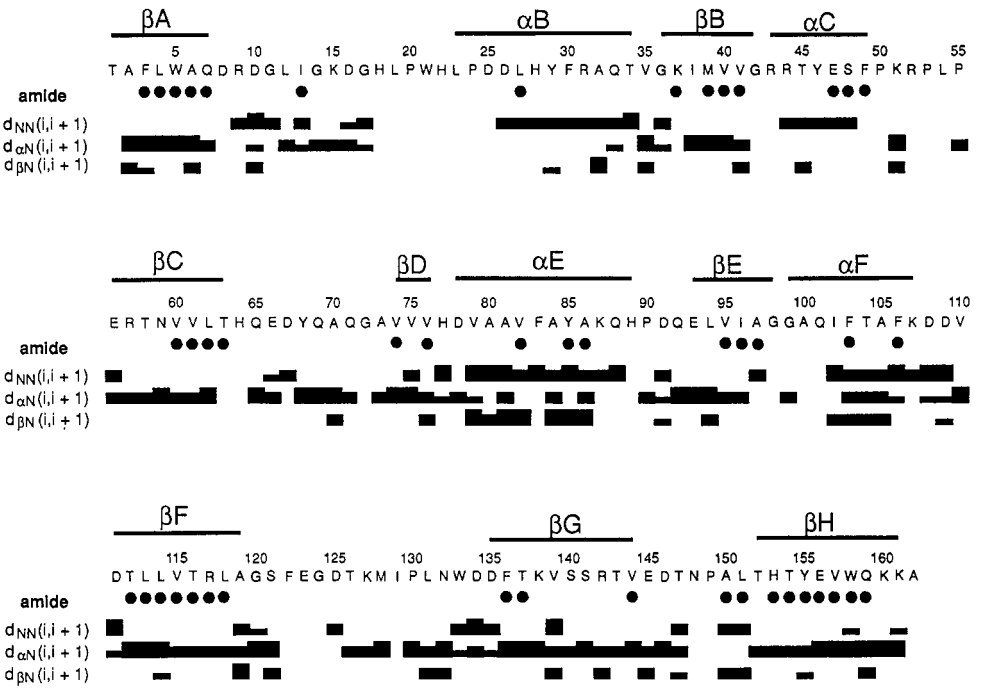

FIGURE 5: Summary of the sequential NOEs identified for the DHFR·MTX complex. The height of the bar used to denote an NOE is an indication of its intensity. The closed circles below residues denote slowly exchanging amide protons that persist for at least 24 h in D_2O solutions.

than proline for which assignments could not be made in the spectrum of the DHFR·MTX complex are located in turns or loops on the surface of the protein. Hence, if the structure of the DHFR·MTX complex in solution is, as it appears, closely similar to this crystal structure, the observed lack of sequential NOEs involving these residues could be explained by either rapid exchange of the NH proton with water or exchange line-broadening effects related to localized conformational averaging. One exception, however, is leucine 54, where the problem is simply that the residue is sandwiched between two proline residues, which, in the absence of 3D ^{13}C/^{1}H data, act as unbridgeable gaps in the sequential assignments.

(*iii*) *Secondary Structure.* The elements of regular secondary structure in proteins give rise to specific patterns of sequential NOEs. In particular, the extended backbone conformation found in β sheets is characterized by strong αN NOEs, while continuous stretches of five or more residues linked by NN NOEs are very indicative of a helical structure (Wüthrich, 1986).

In the course of making sequential assignments for DHFR·MTX it became apparent that a number of relatively long stretches of the protein sequence were characterized by strong αN NOEs and by slowly exchanging amide protons, specifically residues 2–9, 38–42, 59–63, 92–97, 112–119, 136–146, and 152–162. In addition, a significant number of long-range αCH–NH and NH–NH NOEs were identified, which clearly linked together all but one of these stretches to form a seven-stranded β-sheet. The crystal structure of the DHFR·MTX·NADPH complex contains an eight-stranded β-sheet with the elements aligned as shown in Figure 6 (Bolin et al., 1982) (no crystal structure data is available for the *L. casei* DHFR·MTX complex). The interstrand NOEs observed for DHFR·MTX and the hydrogen bonds implied by the slowly exchanging NHs are both summarized in Figure 6 and clearly show that the main body of this β-sheet is preserved in the binary complex in solution. In addition, long-range NOEs and positions of slowly exchanging amide protons suggest that residues 73–77 form the eighth short strand (strand D) of the β-sheet observed in the crystal structure of

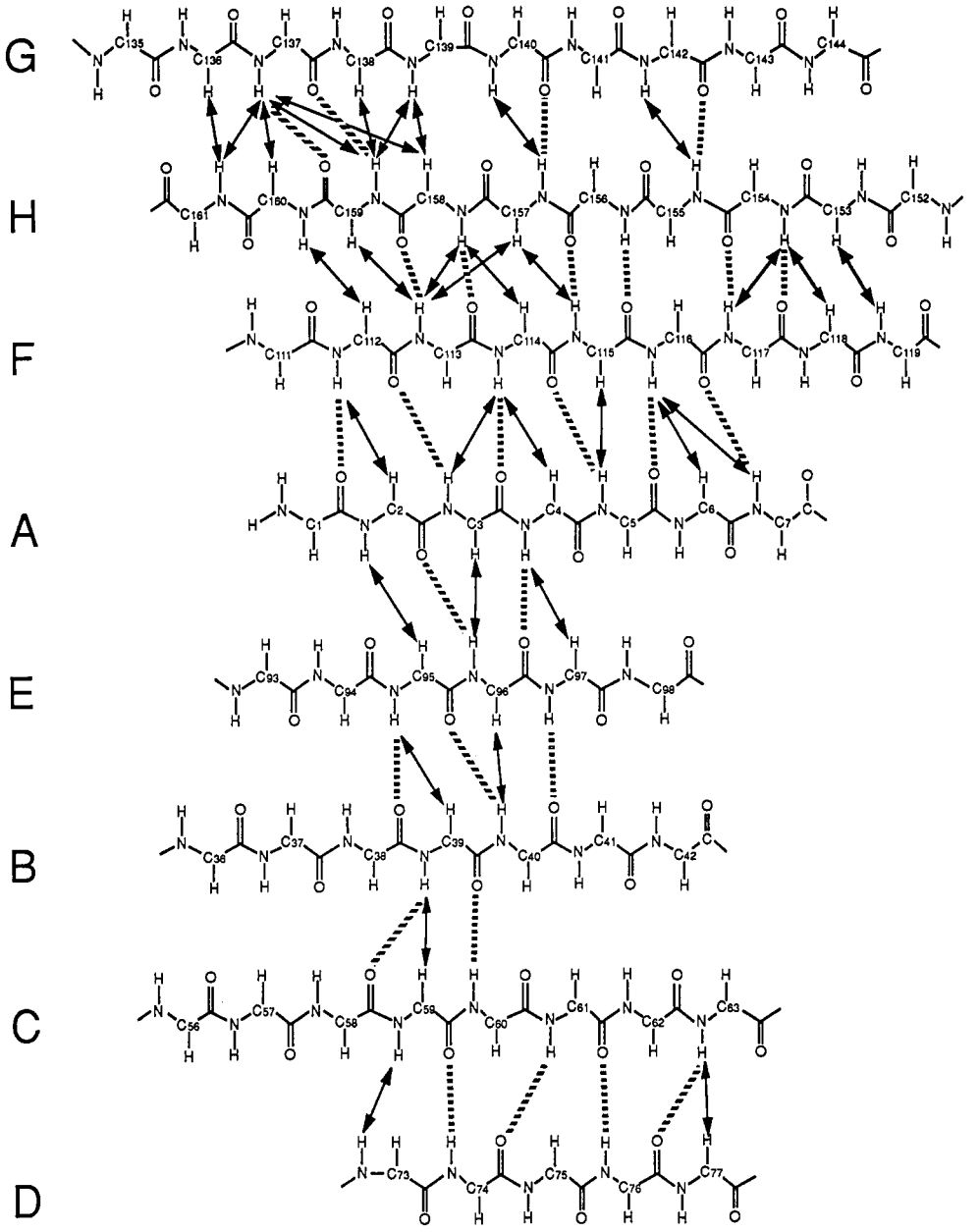

FIGURE 6: Schematic representation of the arrangement of the eight-stranded β-sheet found in the crystal structure of the DHFR·MTX·NADPH complex. The interstrand NOEs observed for DHFR·MTX in solution are represented by the arrows, while hydrogen bonds implied by the observation of slowly exchanging amide protons and NOEs are denoted by the broken lines.

the ternary complex. Thus, the eight-stranded β-sheet, which is such a prominent feature in the crystal structure, remains essentially unaltered in solution.

The sequential NN NOEs observed for the binary DHFR·MTX complex, which are summarized in Figure 5, suggest that residues 26–35, 44–49, 79–89, and 102–110 adopt a helical conformation. Two of these regions, namely, residues 44–49 and 79–89, correspond within one residue to helices C and E, respectively, in the crystal structure of the DHFR·MTX·NADPH complex (Bolin et al., 1982). The helix indicated by the NMR data as involving residues 26–35, however, is about one turn shorter at the N-terminus than helix B in the crystal structure, which spans residues 23–34. Similarly, in the crystal structure helix F encompasses residues 99–107, whereas the corresponding helical region in solution is somewhat offset, comprising amino acids 102–110. It should be noted that the 3D HMQC–NOESY–HMQC and NOESY–HMQC spectra allow us to be sure that particular NN NOEs, predicted by the locations of helices B and F in the crystal structure, are definitely not present, rather than simply not observed due to cross-peak overlap.

The differences in helical structure could be due to crystal packing forces, as both helices are located on the surface of the enzyme, but could also reflect a conformational change in the protein induced by NADPH binding, since the comparison is between the crystal structure of DHFR·MTX·NADPH and the solution structure of DHFR·MTX. In the crystal structure, residues 99, 101, and 102, which are at the N-terminus of helix F, make direct contacts with the bound coenzyme, so a conformational change in this region on NADPH binding is a reasonable possibility. Similarly, although amino acids at the N-terminus of helix B do not interact directly with the bound coenzyme, residues nearby, specifically leucine 19 and tryptophan 21, do make contacts with the nicotinamide moiety and a localized conformational change induced by NADPH binding is again a possibility. This would be consistent with our earlier findings, based on coenzyme-induced chemical shift changes, that the loop com-

prising residues 13–23 undergoes a conformational change on coenzyme binding (Hammond et al., 1986). The case for an NADPH-induced conformational change accounting for the local differences in structure is perhaps strengthened by the fact that only one sequential NOE between residues in the "missing" helical regions could be identified. This may be indicative of some sort of localized conformational averaging, i.e., flexibility, in these areas of the structure in the binary DHFR·MTX complex. Detailed confirmation of any coenzyme-induced conformational changes will have to await the sequential assignment of the spectrum of the DHFR·MTX·NADPH complex.

Conclusions

Before advances in instrumentation and experimental methods opened up the possibility of obtaining essentially complete sequential assignments for relatively large proteins, such as DHFR, our previous studies had relied on making assignments by comparing the NOEs observed in spectra from several enzyme·ligand complexes with those predicted from the DHFR·MTX·NADPH crystal structure (Hammond et al., 1986; Birdsall et al., 1990a). The limitations of this assignment method are that a high-resolution crystal structure of the protein must be available and the conformation in the crystal and in solution must be similar. However, it is worth noting that in the case of DHFR all the previous assignments based on correlating NOE and X-ray data have been confirmed by the present work. This indicates that the crystal and solution structures are indeed similar, a conclusion fully supported by direct comparison of the secondary structure found in the crystal with that determined in solution by this study. Small differences between the crystal and solution structures would usually not lead to errors in resonance assignments based on the crystal structure, since this involves a qualitative comparison of predicted and observed NOEs. The NOEs used in such assignments often relate to interproton distances of $\sim 4.5 \pm 0.5$ Å; since a 5-Å NOE will be 25% the intensity expected for a 4-Å NOE, it would still be sufficient to establish the connections between the side-chain protons.

In order to use NMR spectroscopy to define structural differences between complexes formed with different ligands, it will be necessary to transfer the assignments for the binary DHFR·MTX complex reported here to the ^{1}H spectra of other complexes. Preliminary studies on other binary and ternary complexes indicate that most assignments will be easily transferable by using conventional 2D NOESY, COSY, and HOHAHA spectra. This is because many signals in the protein spectra remain relatively unchanged between complexes and those that do change can usually be monitored with ease because of the similarities in the overall connectivity patterns in the 2D spectra. In addition, for some relatively well-resolved signals with markedly different chemical shifts in different complexes, assignments can be transferred by 2D exchange experiments [e.g., Hammond et al. (1986)]. However, in order to define long-range NOEs required for determining detailed structural information, it will still be necessary to examine 3D heteronuclear spectra of ^{15}N- or ^{13}C-labeled protein to achieve the required resolution of normally overlapping cross peaks.

The assignments reported here represent a significant step forward in the NMR studies of DHFR. In particular, they will allow a more detailed interpretation of the ligand binding and site-directed mutagenesis work currently in progress (Birdsall et al., 1989a; Jimenez et al., 1989) by allowing us to use NOE data to define structural changes in the enzyme·ligand complexes. In addition, the procedure used to obtain sequential assignments for DHFR·MTX, in conjunction with similar work on interleukin 1β (Marion et al., 1989; Driscoll et al., 1990) and calmodulin (Ikura et al., 1990), gives some pointers as to how to approach the problem of sequential assignment and subsequent structural determination of proteins with molecular weights in the range 25 000–30 000 Da.

Acknowledgments

The NMR spectra were recorded by using facilities at the Medical Research Council Biomedical NMR Centre, NIMR, Mill Hill. We thank Mrs. G. Ostler for expert technical assistance.

Registry No. DHFR, 9002-03-3.

References

Andrews, J., Clore, G. M., Davies, R. W., Gronenborn, A. M., Gronenborn, B., Kalderon, D., Papadopoulos, P. C., Schafer, S., Sims, P. F. G., & Stancombe, R. (1985) *Gene 35*, 217–222.

Bax, A., & Davis, D. G. (1985) *J. Magn. Reson. 65*, 355–360.

Bax, A., Griffey, R. H., & Hawkins, B. L. (1983) *J. Am. Chem. Soc. 105*, 7188–7190.

Bax, A., Clore, G. M., Driscoll, P. C., Gronenborn, A. M., Ikura, M., & Kay, L. E. (1990a) *J. Magn. Reson. 87*, 620–627.

Bax, A., Clore, G. M., & Gronenborn, A. M. (1990b) *J. Magn. Reson. 88*, 425–431.

Birdsall, B., Andrews, J., Ostler, G., Tendler, S. J., Feeney, J., Roberts, G. C. K., Davies, R. W., & Cheung, H. T. (1989a) *Biochemistry 28*, 1353–1362.

Birdsall, B., Feeney, J., Tendler, S. J. B., Hammond, S. J., & Roberts, G. C. K. (1989b) *Biochemistry 28*, 2297–2305.

Birdsall, B., Arnold, J. R. P., Jimenez-Barbero, J., Frenkiel, T. A., Bauer, C. J., Tendler, S. J. B., Carr, M. D., Thomas, J. A., Roberts, G. C. K., & Feeney, J. (1990a) *Eur. J. Biochem. 191*, 659–668.

Birdsall, B., Tendler, S. J. B., Arnold, J. R. P., Feeney, J., Griffin, R. J., Carr, M. D., Thomas, J. A., Roberts, G. C. K., & Stevens, M. F. G. (1990b) *Biochemistry 29*, 9660–9667.

Blakley, R. L. (1985) in *Folates and Pterins* (Blakley, R. L., & Benkovic, S. J., Eds.) Vol. 1, Chapter 5, pp 191–253, Wiley, New York.

Bolin, J. T., Filman, D. J., Matthews, D. A., Hamlin, R. C., & Kraut, J. (1982) *J. Biol. Chem. 257*, 13650–13662.

Braunschweiler, L., & Ernst, R. R. (1983) *J. Magn. Reson. 53*, 521–528.

Breg, J. N., Boelens, R., George, A. V. E., & Kaptein, R. (1989) *Biochemistry 28*, 9826–9833.

Brown, S. C., Weber, P. L., & Mueller, L. (1988) *J. Magn. Reson. 77*, 166–169.

Carver, J. A., Cooke, R. M., Esposito, G., Campbell, I. D., Gregory, H., & Sheard, B. (1986) *FEBS Lett. 205*, 77–81.

Clore, G. M., Appella, E., Yamada, M., Matsushima, K., & Gronenborn, A. M. (1989) *J. Biol. Chem. 264*, 18907–18911.

Dann, J. G., Ostler, G., Bjur, R. A., King, R. W., Scudder, P., Turner, P. C., Roberts, G. C. K., & Burgen, A. S. V. (1976) *Biochem. J. 157*, 559–571.

Davis, D. G., & Bax, A. (1985) *J. Am. Chem. Soc. 107*, 2820–2821.

Driscoll, P. C., Clore, G. M., Marion, D., Wingfield, P. T., & Gronenborn, A. M. (1990) *Biochemistry 29*, 3542–3556.

Feeney, J. (1990) *Biochem. Pharmacol. 40*, 141–152.

Feeney, J., Birdsall, B., Ostler, G., Carr, M. D., & Kairi, M. (1990) *FEBS Lett. 272*, 197–199.
Fesik, S. W., & Zuiderweg, E. R. P. (1990) *Q. Rev. Biophys. 23*, 97–131.
Freisheim, J. H., & Matthews, D. A. (1984) in *Folate Antagonists as Chemotherapeutic Agents* (Sirotnak, F. M., Burchall, J. J., Ensminger, W. B., & Montgomery, J. A., Eds.) Vol. 1, pp 69–131, Academic Press, New York.
Frenkiel, T., Bauer, C. J., Carr, M. D., Birdsall, B., & Feeney, J. (1990) *J. Magn. Reson. 90*, 420–425.
Hammond, S. J., Birdsall, B., Searle, M. S., Roberts, G. C. K., & Feeney, J. (1986) *J. Mol. Biol. 188*, 81–97.
Ikura, M., Kay, L. E., & Bax, A. (1990) *Biochemistry 29*, 4659–4667.
Jeener, J., Meier, B. H., Bachmann, P., & Ernst, R. R. (1979) *J. Chem. Phys. 71*, 4546–4553.
Jimenez, M. A., Arnold, J. R. P., Andrews, J., Thomas, J. A., Roberts, G. C. K., Birdsall, B., & Feeney, J. (1989) *Protein Eng. 2*, 627–631.
Kuyper, L. F., Roth, B., Baccanari, D. P., Ferone, R., Beddell, C. R., Champness, J. N., Stammers, D. K., Dann, J. G., Norrington, F. E. A., Baker, D. J., & Goodford, P. J. (1982) *J. Med. Chem. 25*, 1120–1122.
Llinas, M., Wilson, D. M., & Klein, M. P. (1977) *J. Am. Chem. Soc. 99*, 6846–6849.
Macura, S., Huong, Y., Suter, D., & Ernst, R. R. (1981) *J. Magn. Reson. 43*, 259–281.
Marion, D., & Wüthrich, K. (1983) *Biochem. Biophys. Res. Commun. 113*, 967–974.
Marion, D., Driscoll, P. C., Kay, L. E., Wingfield, P. T., Bax, A., Gronenborn, A. M., & Clore, G. M. (1989a) *Biochemistry 28*, 6150–6156.
Marion, D., Kay, L. E., Sparks, S. W., Torchia, D. A., & Bax, A. (1989b) *J. Am. Chem. Soc. 111*, 1515–1517.
McIntosh, L. P., Griffey, R. H., Muchmore, D. C., Nielson, C. P., Redfield, A. G., & Dahlquist, F. W. (1987) *Proc. Natl. Acad. Sci. U.S.A. 84*, 1244–1248.
Morris, G. A., & Freeman, R. (1978) *J. Magn. Reson. 29*, 433–462.
Mueller, L. (1979) *J. Am. Chem. Soc. 101*, 4481–4484.
Niemczura, W. P., Helms, G. L., Chesnick, A. S., Moore, R. E., & Bornemann, V. (1989) *J. Magn. Reson. 81*, 635–640.
Rance, M., Sorensen, O. W., Bodenhausen, G., Wagner, G., Ernst, R. R., & Wüthrich, K. (1983) *Biochem. Biophys. Res. Commun. 117*, 479–485.
Redfield, C., & Dobson, C. M. (1988) *Biochemistry 27*, 122–136.
Roberts, G. C. K. (1990) in *Chemistry and Biology of Pteridines (1989)* (Curtius, H.-C., Ghisla, S., & Blau, N., Ed.) pp 681–693, De Gruyter, Berlin.
Senn, H., Otting, G., & Wüthrich, K. (1987) *J. Am. Chem. Soc. 109*, 1090–1092.
Stockman, B. J., Reilly, M. D., Westler, W. M., Ulrich, E. L., & Markley, J. L. (1989) *Biochemistry 28*, 230–236.
Strop, P., Wider, G., & Wüthrich, K. (1983) *J. Mol. Biol. 166*, 641–667.
Torchia, D. A., Sparks, S. W., & Bax, A. (1989) *Biochemistry 28*, 5509–5524.
Wagner, G., & Wüthrich, K. (1982) *J. Mol. Biol. 155*, 347–366.
Westler, W. M., Stockman, B. J., Markley, J. L., Hosoya, Y., Miyake, Y., & Kainosho, M. (1988) *J. Am. Chem. Soc. 110*, 6256–6258.
Widmer, H., Wagner, G., Schweitz, H., Lazdunski, M., & Wüthrich, K. (1988) *Eur. J. Biochem. 171*, 177–192.
Wüthrich, K. (1986) *NMR of Proteins and Nucleic Acids*, Wiley, New York.
Zuiderweg, E. R. P., & Fesik, S. W. (1989) *Biochemistry 28*, 2387–2391.
Zuiderweg, E. R. P., McIntosh, L. P., Dahlquist, F. W., & Fesik, S. W. (1990) *J. Magn. Reson. 86*, 210–216.